

An improved measurement of $B^0-\bar{B}^0$ mixing in Z^0 decays

L3 Collaboration

B. Adeva^a, O. Adriani^b, M. Aguilar-Benitez^c, S. Ahlen^d, H. Akbari^e, J. Alcaraz^a, A. Aloisio^f, G. Alverson^g, M.G. Alviggi^f, G. Ambrosi^h, Q. Anⁱ, H. Anderhub^j, A.L. Anderson^k, V.P. Andreev^l, T. Angelov^k, L. Antonov^m, D. Antreasyanⁿ, P. Arce^c, A. Arefiev^o, A. Atamanchuk^l, T. Azemoun^p, T. Aziz^{q,r}, P.V.K.S. Babaⁱ, P. Bagnaia^s, J.A. Bakken^t, L. Baksay^u, R.C. Ball^p, S. Banerjee^q, J. Bao^e, R. Barillere^a, L. Barone^s, R. Battiston^h, A. Bay^v, F. Becattini^b, U. Becker^{k,j}, F. Behner^j, J. Behrens^j, S. Beingessner^w, Gy.L. Bencze^x, J. Berdugo^c, P. Berges^k, B. Bertucci^h, B.L. Betev^{m,j}, M. Biasini^h, A. Biland^j, G.M. Bilei^h, R. Bizzarri^s, J.J. Blaising^w, B. Blumenfeld^e, G.J. Bobbink^{a,y}, M. Bocciolini^b, R. Bock^r, A. Böhm^r, B. Borgia^s, D. Bourilkov^z, M. Bourquin^v, D. Boutigny^w, B. Bouwens^y, E. Brambilla^f, J.G. Branson^{aa}, I.C. Brock^{ab}, M. Brooks^{ac}, C. Buisson^{ad}, A. Bujak^{ae}, J.D. Burger^k, W.J. Burger^v, J.P. Burq^{ad}, J. Busenitz^u, X.D. Caiⁱ, M. Capell^{af}, M. Caria^h, G. Carlino^f, F. Carminati^b, A.M. Cartacci^b, M. Cerrada^c, F. Cesaroni^s, Y.H. Chang^k, U.K. Chaturvediⁱ, M. Chemarin^{ad}, A. Chen^{ag}, C. Chen^{ah}, G.M. Chen^{ah}, H.F. Chen^{ai}, H.S. Chen^{ah}, J. Chen^k, M. Chen^k, M.L. Chen^p, W.Y. Chenⁱ, G. Chiefari^f, C.Y. Chien^e, M. Chmeissani^p, S. Chung^k, C. Civinini^b, I. Clare^k, R. Clare^k, T.E. Coan^{ac}, H.O. Cohn^{aj}, G. Coignet^w, N. Colino^a, A. Continⁿ, F. Crijns^z, X.T. Cuiⁱ, X.Y. Cuiⁱ, T.S. Dai^k, R. D'Alessandro^b, R. de Asmundis^f, A. Degré^w, K. Deiters^k, E. Dénes^x, P. Denes^t, F. DeNotaristefani^s, M. Dhina^j, D. DiBitonto^u, M. Diemoz^s, H.R. Dimitrov^m, C. Dionisi^{sa}, M.T. Dovaⁱ, E. Drago^f, T. Driever^z, D. Duchesneau^v, P. Duinker^y, H. El Mamouni^{ad}, A. Engler^{ab}, F.J. Epling^k, F.C. Erné^y, P. Extermann^v, R. Fabbretti^{ak}, M. Fabre^{ak}, S. Falciano^s, S.J. Fan^{al}, O. Fackler^{af}, J. Fay^{ad}, M. Felcini^a, T. Ferguson^{ab}, D. Fernandez^c, G. Fernandez^c, F. Ferroni^s, H. Fesefeldt^r, E. Fiandrini^h, J. Field^v, F. Filthaut^z, G. Finocchiaro^s, P.H. Fisher^e, G. Forconi^v, T. Foreman^y, K. Freudenreich^j, W. Friebel^{am}, M. Fukushima^k, M. Gailloud^{an}, Yu. Galaktionov^{o,k}, E. Gallo^b, S.N. Ganguli^q, P. Garcia-Abia^c, S.S. Gau^{ag}, D. Gele^{ad}, S. Gentile^{sa}, S. Goldfarb^p, Z.F. Gong^{ai}, E. Gonzalez^c, P. Göttlicher^r, A. Gougas^e, D. Goujon^v, G. Gratta^{ao}, C. Grinnell^k, M. Gruenewald^{ao}, C. Guⁱ, M. Guanziroliⁱ, J.K. Guo^{al}, V.K. Gupta^t, A. Gurtu^{a,q}, H.R. Gustafson^p, L.J. Gutay^{ae}, K. Hangarter^r, A. Hasanⁱ, D. Hauschildt^y, C.F. He^{al}, T. Hebbeker^r, M. Hebert^{aa}, G. Herten^k, U. Herten^r, A. Hervé^a, K. Hilgers^r, H. Hofer^j, H. Hoorani^v, G. Huⁱ, G.Q. Hu^{al}, B. Ille^{ad}, M.M. Ilyasⁱ, V. Innocente^{af}, H. Janssen^a, S. Jezequel^w, B.N. Jin^{ah}, L.W. Jones^p, A. Kasser^{an}, R.A. Khanⁱ, Yu. Kamyshkov^{aj}, P. Kapinos^l, J.S. Kapustinsky^{ac}, Y. Karyotakis^{aw}, M. Kaurⁱ, S. Khokharⁱ, M.N. Kienzle-Focacci^v, W.W. Kinnison^{ac}, D. Kirkby^{ao}, S. Kirsch^{am}, W. Kittel^z, A. Klimentov^{ko}, A.C. König^z, E. Koffeman^y, O. Kornadt^r, V. Koutsenko^{ko}, A. Koulbardis^l, R.W. Kraemer^{ab}, T. Kramer^k, V.R. Krastev^{m,h}, W. Krenz^r, A. Krivshich^l, K.S. Kumar^{ap}, A. Kunin^{ap,o}, G. Landi^b, D. Lanske^r, S. Lanzano^w, P. Lebrun^{ad}, P. Lecomte^j, P. Lecoq^a, P. Le Coultre^j, D.M. Lee^{ac}, I. Leedom^g, J.M. Le Goff^a, R. Leiste^{am}, M. Lenti^b, E. Leonardi^s, J. Lettry^j, X. Leytens^y, C. Li^{ai,i}, H.T. Li^{ah}, P.J. Li^{al}, X.G. Li^{ah}, J.Y. Liao^{al}, W.T. Lin^{ag}, Z.Y. Lin^{ai}, F.L. Linde^{ay}, B. Lindemann^r, D. Linnhofer^j, L. Lista^f, Y. Liuⁱ, W. Lohmann^{am,a}, E. Longo^s, Y.S. Lu^{ah}, J.M. Lubbers^a, K. Lübelmeyer^r, C. Luci^s, D. Luckey^{n,k}, L. Ludovici^s,

L. Luminari^s, W.G. Ma^{ai}, M. MacDermott^j, P.K. Malhotra^{q,l}, R. Malikⁱ, A. Malinin^{w,o}, C. Maña^c, D.N. Mao^p, Y.F. Mao^{ah}, M. Maolinbay^j, P. Marchesini^j, F. Marion^w, A. Marin^d, J.P. Martin^{ad}, L. Martinez-Laso^a, F. Marzano^s, G.G.G. Massaro^y, T. Matsuda^k, K. Mazumdar^q, P. McBride^{ap}, T. McMahon^{ae}, D. McNally^j, Th. Meinholz^r, M. Merk^z, L. Merola^f, M. Meschini^b, W.J. Metzger^z, Y. Miⁱ, G.B. Mills^{ac}, Y. Mirⁱ, G. Mirabelli^s, J. Mnich^r, M. Möller^r, B. Monteleoni^b, R. Morand^w, S. Morganti^s, N.E. Moulaiⁱ, R. Mount^{ao}, S. Müller^r, A. Nadtochy^l, E. Nagy^x, M. Napolitano^f, H. Newman^{ao}, C. Neyer^j, M.A. Niazⁱ, A. Nippe^r, H. Nowak^{am}, G. Organtini^s, D. Pandoulas^r, S. Paoletti^b, P. Paolucci^f, G. Passaleva^{b,h}, S. Patricelli^f, T. Paul^e, M. Pauluzzi^h, F. Pauss^j, Y.J. Pei^r, D. Perret-Gallix^w, J. Perrier^v, A. Pevsner^e, D. Piccolo^f, M. Pieri^{ab}, P.A. Piroué^t, F. Plasil^{aj}, V. Plyaskin^o, M. Pohl^j, V. Pojidaev^{ob}, N. Produit^v, J.M. Qian^p, K.N. Qureshiⁱ, R. Raghavan^q, G. Rahal-Callot^j, G. Raven^y, P. Raziš^{aq}, K. Read^{aj}, D. Ren^j, Z. Renⁱ, M. Rescigno^s, S. Reucroft^g, A. Ricker^r, S. Riemann^{am}, O. Rind^p, H.A. Rizviⁱ, B.P. Roe^p, M. Röhner^r, S. Röhner^r, L. Romero^c, J. Rose^r, S. Rosier-Lees^w, R. Rosmalen^z, Ph. Rosselet^{an}, A. Rubbia^k, J.A. Rubio^{ac}, H. Rykaczewski^j, M. Sachwitz^{am}, E. Sajan^h, J. Salicio^{ac}, J.M. Salicio^c, G.S. Sanders^{ac}, A. Santocchia^h, M.S. Sarakinos^k, G. Sartorelli^{n,i}, M. Sassowsky^r, G. Sauvage^w, V. Schegelsky^l, K. Schmiemann^r, D. Schmitz^r, P. Schmitz^r, M. Schneegans^w, H. Schopper^{ar}, D.J. Schotanus^z, S. Shotkin^k, H.J. Schreiber^{am}, J. Shukla^{ab}, R. Schulte^r, S. Schulte^r, K. Schultze^r, J. Schütte^{ap}, J. Schwenke^r, G. Schwering^r, C. Sciacca^f, I. Scott^{ap}, R. Sehgalⁱ, P.G. Seiler^{ak}, J.C. Sens^{a,y}, L. Servoli^h, I. Sheer^{aa}, D.Z. Shen^{al}, S. Shevchenko^{ao}, X.R. Shi^{ao}, E. Shumilov^o, V. Shoutko^o, E. Soderstrom^t, A. Sopczak^{aa}, C. Spartiotis^e, T. Spickermann^r, P. Spillantini^b, R. Starosta^r, M. Steuer^{n,k}, D.P. Stickland^t, F. Sticozzi^k, H. Stone^v, K. Strauch^{ap}, B.C. Stringfellow^{ae}, K. Sudhakar^{q,r}, G. Sultanovⁱ, R.L. Sumner^t, L.Z. Sun^{ai,i}, H. Suter^j, R.B. Sutton^{ab}, J.D. Swainⁱ, A.A. Syedⁱ, X.W. Tang^{ah}, L. Taylor^g, C. Timmermans^z, Samuel C.C. Ting^k, S.M. Ting^k, M. Tonutti^r, S.C. Tonwar^q, J. Tóth^x, A. Tsaregorodtsev^l, G. Tsipolitis^{ab}, C. Tully^{ao}, K.L. Tung^{ah}, J. Ulbricht^j, L. Urbán^x, U. Uwer^r, E. Valente^s, R.T. Van de Walle^z, I. Vetlitsky^o, G. Viertel^j, P. Vikasⁱ, U. Vikasⁱ, M. Vivargent^w, H. Vogel^{ab}, H. Vogt^{am}, I. Vorobiev^o, A.A. Vorobyov^l, L. Vuilleumier^{an}, M. Wadhwaⁱ, W. Wallraff^r, C.R. Wang^{ai}, G.H. Wang^{ab}, J.H. Wang^{ah}, Q.F. Wang^{ap}, X.L. Wang^{ai}, Y.F. Wang^b, Z.M. Wang^{i,ai}, A. Weber^r, J. Weber^j, R. Weill^{an}, T.J. Wenaus^{af}, J. Wenninger^v, M. White^k, C. Willmott^c, F. Wittgenstein^a, D. Wright^t, R.J. Wu^{ah}, S.X. Wuⁱ, Y.G. Wu^{ah}, B. Wysłouch^k, Y.Y. Xie^{al}, Y.D. Xu^{ah}, Z.Z. Xu^{ai}, Z.L. Xue^{al}, D.S. Yan^{al}, X.J. Yan^k, B.Z. Yang^{ai}, C.G. Yang^{ah}, G. Yangⁱ, K.S. Yang^{ah}, Q.Y. Yang^{ah}, Z.Q. Yang^{al}, C.H. Yeⁱ, J.B. Ye^{ai}, Q. Yeⁱ, S.C. Yeh^{ag}, Z.W. Yin^{al}, J.M. Youⁱ, N. Yunusⁱ, M. Yzerman^y, C. Zaccardelli^{ao}, P. Zemp^j, M. Zengⁱ, Y. Zeng^r, D.H. Zhang^y, Z.P. Zhang^{ai,i}, B. Zhou^d, J.F. Zhou^r, R.Y. Zhu^{ao}, H.L. Zhuang^{ah}, A. Zichichi^{n,ai} and B.C.C. van der Zwaan^y

^a European Laboratory for Particle Physics, CERN, CH-1211 Geneva 23, Switzerland

^b INFN – Sezione di Firenze and Università di Firenze, I-50125 Florence, Italy

^c Centro de Investigaciones Energeticas, Medioambientales y Tecnologicas, CIEMAT, E-28040 Madrid, Spain

^d Boston University, Boston, MA 02215, USA

^e Johns Hopkins University, Baltimore, MD 21218, USA

^f INFN – Sezione di Napoli and Università di Napoli, I-80125 Naples, Italy

^g Northeastern University, Boston, MA 02115, USA

^h INFN – Sezione di Perugia and Università Degli Studi di Perugia, I-06100 Perugia, Italy

ⁱ World Laboratory, FBLJA Project, CH-1211 Geneva 23, Switzerland

^j Eidgenössische Technische Hochschule, ETH Zürich, CH-8093 Zurich, Switzerland

^k Massachusetts Institute of Technology, Cambridge, MA 02139, USA

^l Nuclear Physics Institute, St. Petersburg, Russian Federation

- ^m *Bulgarian Academy of Sciences, Institute of Mechatronics, BU-1113 Sofia, Bulgaria*
ⁿ *INFN – Sezione di Bologna, I-40126 Bologna, Italy*
^o *Institute of Theoretical and Experimental Physics, ITEP, 117 259 Moscow, Russian Federation*
^p *University of Michigan, Ann Arbor, MI 48109, USA*
^q *Tata Institute of Fundamental Research, Bombay 400 005, India*
^r *I. Physikalisches Institut, RWTH, W-5100 Aachen, FRG²*
and III. Physikalisches Institut, RWTH, W-5100 Aachen, FRG²
^s *INFN – Sezione di Roma and Università di Roma “La Sapienza”, I-00185 Rome, Italy*
^t *Princeton University, Princeton, NJ 08544, USA*
^u *University of Alabama, Tuscaloosa, AL 35486, USA*
^v *University of Geneva, CH-1211 Geneva 4, Switzerland*
^w *Laboratoire de Physique des Particules, LAPP, F-74941 Annecy-le-Vieux, France*
^x *Central Research Institute for Physics of the Hungarian Academy of Sciences, H-1525 Budapest 114, Hungary*
^y *National Institute for High Energy Physics, NIKHEF, NL-1009 DB Amsterdam, The Netherlands*
^z *University of Nijmegen and NIKHEF, NL-6525 ED Nijmegen, The Netherlands*
^{aa} *University of California, San Diego, CA 92182, USA*
^{ab} *Carnegie Mellon University, Pittsburgh, PA 15213, USA*
^{ac} *Los Alamos National Laboratory, Los Alamos, NM 87544, USA*
^{ad} *Institut de Physique Nucléaire de Lyon, IN2P3-CNRS/Université Claude Bernard, F-69622 Villeurbanne Cedex, France*
^{ae} *Purdue University, West Lafayette, IN 47907, USA*
^{af} *Lawrence Livermore National Laboratory, Livermore, CA 94550, USA*
^{ag} *High Energy Physics Group, Taiwan, ROC*
^{ah} *Institute of High Energy Physics, IHEP, Beijing, China*
^{ai} *Chinese University of Science and Technology, USTC, Hefei, Anhui 230 029, China*
^{aj} *Oak Ridge National Laboratory, Oak Ridge, TN 37830, USA*
^{ak} *Paul Scherrer Institut, PSI, CH-5232 Villigen, Switzerland*
^{al} *Shanghai Institute of Ceramics, SIC, Shanghai, China*
^{am} *Institut für Hochenergiephysik, O-1615 Zeuthen, FRG²*
^{an} *University of Lausanne, CH-1015 Lausanne, Switzerland*
^{ao} *California Institute of Technology, Pasadena, CA 91125, USA*
^{ap} *Harvard University, Cambridge, MA 02139, USA*
^{aq} *Department of Natural Sciences, University of Cyprus, Nicosia, Cyprus*
^{ar} *University of Hamburg, W-2000 Hamburg, FRG*

Received 18 May 1992

A more precise determination of the $B^0-\bar{B}^0$ mixing parameter in Z^0 decays based on a fourfold increase in statistics has been made using the 1990 and 1991 L3 data. The analysis of the dilepton events, muons and electrons, gives: $\chi_B = 0.121 \pm 0.017$ (stat) ± 0.006 (sys). Using the value of χ_d measured at the $\Upsilon(4S)$ we derive the following limit for χ_s : $\chi_s > 0.16$ (90% CL).

1. Introduction

In the standard model the transformation of a B_d^0 or B_s^0 meson into its antiparticle proceeds via a weak flavor-changing box diagram, dominated by virtual top quark exchange. The rate of mixing depends on

the Cabibbo–Kobayashi–Maskawa matrix elements, V_{td} and V_{ts} , and the top quark mass. The semi-leptonic decay modes allow b-hadrons to be tagged since the lepton generally has a high momentum p , due to the hard fragmentation, and a large momentum transverse with respect to the b-quark direction, p_\perp , due to the high b-quark mass. A distinctive experimental signature of $B^0-\bar{B}^0$ mixing is the observation of like sign dileptons from the decays $B^0 \rightarrow \ell^+$ and $\bar{B}^0 \rightarrow B^0 \rightarrow \ell^+$. The amount of mixing may be expressed as

¹ Deceased.

² Supported by the German Bundesministerium für Forschung und Technologie.

$$\chi_B = \frac{\text{Br}(b \rightarrow \bar{B}^0 \rightarrow B^0 \rightarrow \ell + X)}{\text{Br}(b \rightarrow b\text{-hadron} \rightarrow \ell \pm X)},$$

assuming equal semi-leptonic branching ratios for all hadrons containing a b-quark. Measurements of χ_B at the Z^0 resonance are sensitive to both B_d^0 and B_s^0 mixing, i.e. $\chi_B = f_d \chi_d + f_s \chi_s$, where χ_d and χ_s are the mixing parameters and f_d and f_s are the production fractions of B_d^0 and B_s^0 mesons. Previous measurements of the χ_B parameter have been made at proton colliders [1-3] and at e^+e^- colliders at the $\Upsilon(4S)$ [4-6] as well as at the Z^0 [7-10]. At the $\Upsilon(4S)$ no B_s^0 mesons are produced, thus allowing a direct measurement of χ_d .

In a previous paper the L3 Collaboration reported a measurement of $B^0-\bar{B}^0$ mixing [7]. This measurement was performed using a data sample of 5.5 pb^{-1} , which had been accumulated in 1989 and 1990 at $\sqrt{s} \approx M_{Z^0}$. During 1991 an additional 12 pb^{-1} was collected. Our total sample corresponds to 410 000 hadronic decays of the Z^0 . The data have been taken at center-of-mass energies in the range $88.2 \leq \sqrt{s} \leq 94.2 \text{ GeV}$. For this paper we combined the data taken in 1990 and 1991 which represent a fourfold increase in statistics. This allows us to perform a more precise measurement of the $B^0-\bar{B}^0$ mixing and to study in more detail systematic effects. The 1989 data have not been used.

2. The L3 detector

The L3 detector covers 99% of 4π . The detector consists of a central tracking chamber, a high resolution electromagnetic calorimeter composed of BGO crystals, a ring of scintillation counters, a uranium and brass hadron calorimeter with proportional wire chamber readout, and a precise muon chamber system. These detectors are installed in a 12 m diameter magnet which provides a uniform field of 0.5 T along the beam direction.

The central tracking chamber is a time expansion chamber which consists of 2 cylindrical layers of 12 and 24 sectors, with 62 wires measuring the $R-\phi$ coordinate. The average single wire resolution is $58 \mu\text{m}$ over the entire cell. The double-track resolution is $640 \mu\text{m}$. The fine segmentation of the BGO detector and the hadron calorimeter allow us to measure the direction of jets with an angular resolution of 2.5° , and to

measure the total energy of hadronic events from Z^0 decay with a resolution of 10.2%. The muon detector consists of 3 layers of precise drift chambers, which measure the muon trajectory 56 times in the bending plane, and 8 times in the non-bending direction.

For the present analysis, we use the data collected in the following ranges of polar angles:

- for the central chamber, $41^\circ < \theta < 139^\circ$,
- for the hadron calorimeter, $5^\circ < \theta < 175^\circ$,
- for the muon chambers, $35.8^\circ < \theta < 144.2^\circ$,
- for the electromagnetic calorimeter, $11^\circ < \theta < 169^\circ$.

A detailed description of each detector subsystem, and its performance, is given in ref. [11].

3. Selection of $b\bar{b}$ events

The trigger requirements and the selection criteria for hadronic events containing electrons and muons have been described earlier [7]. Muons are identified and measured in the muon chamber system. We require that a muon track consists of track segments in at least two of the three layers of muon chambers, and that the muon track points to the intersection region. Electrons are identified using the BGO and hadron calorimeters, as well as the central tracking chamber. We require a cluster in the BGO that is consistent with the shape of an electromagnetic shower, as determined from test beam studies [12]. For this analysis, we have only considered electrons in the barrel region ($|\cos\theta| < 0.69$). To reject misidentified hadrons, we require that there be less than 3 GeV deposited in the hadron calorimeter in a cone of half angle 7° behind the electromagnetic cluster. The charge of the electron is determined from the tracking chamber.

The momentum of muon candidates is required to be at least 4 GeV, while the electrons are required to have at least 3 GeV. From a sample of $Z^0 \rightarrow \tau^+\tau^-$ events we have determined the charge confusion to be $0.2 \pm 0.2\%$ for muons and $0.8 \pm 0.3\%$ for electrons.

4. Di-lepton sample

The signature of $B^0-\bar{B}^0$ mixing is hadronic events with two leptons of the same charge on opposite sides

Table 1
The dilepton events in the data.

Charges	$\mu\mu$	ee	$e\mu$	All
$\ell^+\ell^+$ all p_t	167	17	98	282
$\ell^+\ell^+$ $p_t > 1$ GeV	40	14	32	86
$\ell^-\ell^-$ all p_t	110	20	84	214
$\ell^-\ell^-$ $p_t > 1$ GeV	30	12	31	73
$\ell^+\ell^-$ all p_t	458	65	284	807
$\ell^+\ell^-$ $p_t > 1$ GeV	165	51	165	381
$\ell\ell$ all p_t	735	102	466	1303
$\ell\ell$ $p_t > 1$ GeV	235	77	228	540

of the event. The angle between the two leptons is required to be larger than 60° to ensure that both leptons are from different b-hadron decays. The transverse momentum of the leptons is measured with respect to the closest jet, where the jet axis has been determined excluding the lepton from the jet. In our sample there are 1303 inclusive dilepton events; in 540 of these, both leptons have $p_t > 1$ GeV. We have also observed 91 events with three inclusive leptons. They were considered in this analysis by using the two leptons with largest transverse momentum with respect to the nearest jet axis.

The number of events and their distribution in various categories is shown in table 1.

We have simulated hadronic events using the LUND parton shower program JETSET 7.3 [13] with $\Lambda_{LL} = 290$ MeV and string fragmentation and full detector simulation [14]. For the simulation we have used the central values of the experimentally deter-

Table 2

Monte Carlo estimates of the fractions F_i (in %) of various event categories for $p_t > 1$ GeV. X indicates a misidentified hadron or leptons from light hadron decays. The $b \rightarrow \ell$ fraction includes $b \rightarrow \tau \rightarrow \ell$ and $b \rightarrow \bar{c} \rightarrow \ell$ decays.

Category	$\mu\mu$	ee	$e\mu$
1 $b \rightarrow \ell, b \rightarrow \ell$	72.6	79.8	80.9
2 $b \rightarrow c \rightarrow \ell, b \rightarrow c \rightarrow \ell$	0.5	0.0	0.2
3 $b \rightarrow \ell, b \rightarrow c \rightarrow \ell$	16.1	11.2	11.6
4 $b \rightarrow \ell, b \rightarrow X$	7.2	8.2	5.2
5 $b \rightarrow c \rightarrow \ell, b \rightarrow X$	1.0	0.7	1.0
6 $b \rightarrow X, b \rightarrow X$	0.5	0.0	0.4
7 $c \rightarrow \ell, c \rightarrow \ell$	0.8	0.0	0.2
8 X, X	1.3	0.0	0.4

mined semi-leptonic branching ratios and fragmentation parameters of b and c quarks [15,16]: $\text{Br}(b \rightarrow \ell) = 0.117 \pm 0.006$; $\text{Br}(c \rightarrow \ell) = 0.096 \pm 0.006$; $\epsilon_b^z = 0.008$; and $\epsilon_c^z = 0.07$. From Monte Carlo simulation of $Z^0 \rightarrow b\bar{b}$ events we expect that the event sample of table 1 consists mainly of events with two prompt B decays. The estimated fractions from various sources are listed in table 2 for $p_t > 1$ GeV.

5. Results

Three methods have been used to measure the mixing parameter χ_B . One is based on counting the number of high p_t dilepton events with the same charge. We have used two different fitting methods: a four-dimensional fit to the p and p_t spectra of the dileptons, and a factorized two dimensional fit to the p_t and p_t distributions. The first fit uses the full information of the event, but requires large Monte Carlo statistics to accurately determine the probability functions. The second fit has the advantage that single lepton events can be used to determine the probability functions, so fewer Monte Carlo events are needed.

5.1. Counting method

This method is based on the ratio of the number of dilepton events with same charge over all dilepton events requiring $p_t > 1$ GeV for each lepton.

The ratio can be expressed as function of χ_B and the relative fractions F_i as given in table 2 for the 8 event categories:

$$\begin{aligned} \frac{N^{\pm\pm}}{N^{\pm\pm} + N^{+-}} &= 2\chi_B(1-\chi_B)(F_1 + F_2) \\ &+ [\chi_B^2 + (1-\chi_B)^2]F_3 \\ &+ [\chi_B(1-\chi_{\text{back}}) + \chi_{\text{back}}(1-\chi_B)]F_4 \\ &+ [\chi_B\chi_{\text{back}} + (1-\chi_B)(1-\chi_{\text{back}})]F_5 \\ &+ 2\chi_{\text{back}}(1-\chi_{\text{back}})F_6 + P^{\pm\pm}F_8. \end{aligned}$$

The ratio $N^{\pm\pm}/N$ is the sum of the contributions from each sub-sample of the table 2. The mixing parameter χ_B is obtained using the measured value of $N^{\pm\pm}/N$, and the estimations of F_i , χ_{back} and $P^{\pm\pm}$. $P^{\pm\pm}$ is the

Table 3
Systematic errors on χ_B from the counting method.

Contribution	Range of variation	Systematic error
$\text{Br}(b \rightarrow \ell) = 0.117$	± 0.006	0.004
$\text{Br}(c \rightarrow \ell) = 0.096$	± 0.006	0.004
fragmentation parameter		
$\epsilon_b = 0.05$	± 0.006	<0.001
background fraction	$\pm 15\%$	0.002
charge confusion uncertainty	$\pm 0.2\%$	0.002
variation of p_t cut	± 0.25 GeV	0.008
variation in $\Delta p_t/p_t$	$\pm 15\%$	0.003
Monte Carlo statistics		0.008
total		0.013

probability that a pair of fake leptons from non b-quark sources have the same sign. It has been estimated from the Monte Carlo to be 0.54 ± 0.05 . Correlations of fake lepton charges with the initial b-quark charge are accounted for by χ_{back} ,

$$\chi_{\text{back}} = (1 - \chi_B)(1 - c) + \chi_B c,$$

where c is the probability for a fake lepton to have the sign of the b-quark. It has been determined from Monte Carlo studies to be 0.65 ± 0.10 .

The following results have been obtained for $\mu\mu$, ee and $e\mu$ events:

$$\chi_B = 0.089 \pm 0.032 \quad (\mu\mu),$$

$$\chi_B = 0.162 \pm 0.056 \quad (ee),$$

$$\chi_B = 0.103 \pm 0.026 \quad (e\mu),$$

where the errors are statistical only.

The systematic errors have been estimated by varying parameters by their measured or estimated errors. The contributions to the systematic error are shown in table 3. Using a weighted average of the $\mu\mu$, ee , and $e\mu$ results we find

$$\chi_B = 0.104 \pm 0.019 \text{ (stat)} \pm 0.013 \text{ (sys)}.$$

5.2. The four-dimensional fitting method

This fit has been previously described in detail [7]. We summarize here only the important aspects. An unbinned maximum likelihood fit is performed in four dimensions, p and p_t of both leptons. The probability of a data event to come from various sources is

Table 4
Systematic errors from the four-dimensional fit method.

Contribution	Variation	Systematic error
$\text{Br}(b \rightarrow \ell) = 0.117$	± 0.006	0.002
$\text{Br}(c \rightarrow \ell) = 0.096$	± 0.006	0.001
fragmentation parameter		
$\epsilon_b = 0.05$	± 0.006	<0.001
charge confusion uncertainty	$\pm 0.2\%$	0.002
$\Delta p_t/p_t$ variation	$\pm 15\%$	0.003
Monte Carlo statistics		0.008
minimum no. of MC events sampled	30 to 50	0.005
total		0.010

determined by the number and type of Monte Carlo events found in a box having the same average value of $(p_1, p_{t1}, p_2, p_{t2})$ as that data event. From these probabilities, a likelihood function is formed, which is then maximized.

As shown in the tables of systematic error sources, tables 4 and 5 this fit and the factorized fit described below, are less sensitive to changes in branching ratios and background than is the counting method. Because this fit samples Monte Carlo events in four dimensions, a large number of simulated events is needed. Enhanced production of Monte Carlo events with B mesons decaying leptonically helped reduce the error due to Monte Carlo statistics but this is still the dominant source of systematic error in this method. The systematic error quoted for the variation of the box size would also be reduced as the Monte Carlo statistics are increased.

Table 5
Systematic errors from the factorized fit method.

Contribution	Variation	Systematic error
$\text{Br}(b \rightarrow \ell) = 0.117$	± 0.006	0.002
$\text{Br}(c \rightarrow \ell) = 0.096$	± 0.006	0.001
fragmentation parameter		
$\epsilon_b = 0.05$	± 0.006	<0.001
charge confusion uncertainty	$\pm 0.2\%$	0.002
$\Delta p_t/p_t$ variation	$\pm 15\%$	0.003
Monte Carlo statistics		0.008
total		0.006

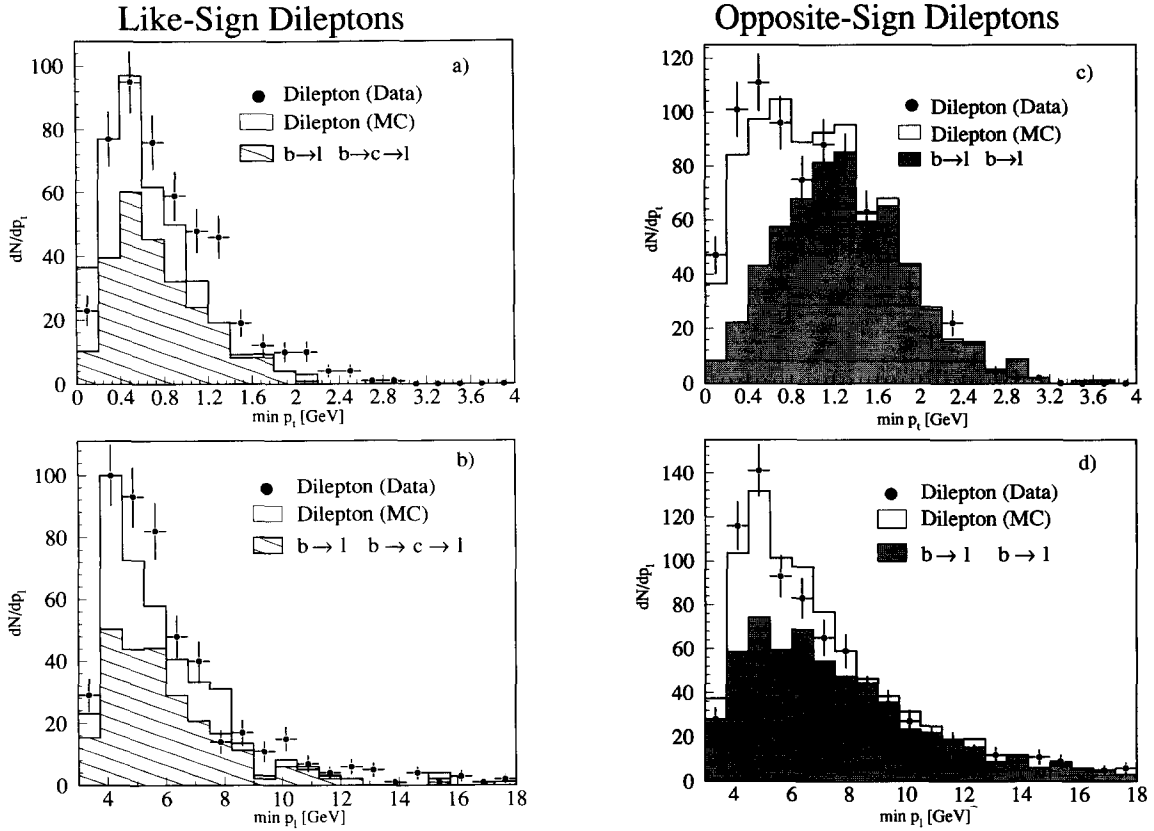


Fig. 1. The minimum p_t and p_ℓ for like sign ((a) and (b)) and opposite sign ((c) and (d)) dilepton events compared to the Monte Carlo expectations with no mixing. The excess of data events in (a) and (b), and the shortage of events in (c) and (d) shows the qualitative effect of mixing.

We determine from this fit

$$\chi_b = 0.124^{+0.018}_{-0.016} \text{ (stat)} \pm 0.010 \text{ (sys)} .$$

5.3. The factorized fit method

In this method, probability functions are assumed to factorize, and are therefore evaluated independently (using the single lepton data and Monte Carlo) for each lepton as a function of p_ℓ and p_t , where p_ℓ is the lepton momentum along the jet axis. Shown in fig. 1 are the p_ℓ and p_t distributions for like sign and opposite sign dileptons.

We define the probability functions for the different lepton sources,

- $b(p)$: probability that the lepton is from prompt $b \rightarrow \ell$,

- $b^\pm(p)$: probability that the lepton (real or fake) is from the decay chain $b \rightarrow X \rightarrow \ell^\pm$ or $\bar{b} \rightarrow X \rightarrow \ell^\mp$;
 $\int (b^+ + b^-) dp = 1$,

- $x(p)$: probability that the lepton (real or fake) is from other sources (u, d, s, c), which are evaluated using the Lund Monte Carlo sample, including the detector simulation, as described above.

A likelihood function is defined

$$L = \prod_{i=1}^{N_{\text{data}}} W_i(p_1, p_2, q_1, q_2),$$

where q_1 and q_2 are the charges of leptons 1 and 2. The weights are:

$$\begin{aligned}
W(p_1, p_2, q_1, q_2) = & \alpha \{ B^2 b(p_1) b(p_2) C(p_1, p_2) U \\
& + B(1-B) [b(p_1) b^+(p_2) + b^+(p_1) b(p_2)] L \\
& + B(1-B) [b(p_1) b^-(p_2) + b^-(p_1) b(p_2)] U \\
& + (1-B)^2 [b^+(p_1) b^+(p_2) + b^-(p_1) b^-(p_2)] U \\
& + (1-B)^2 [b^+(p_1) b^-(p_2) + b^-(p_1) b^+(p_2)] L \} \\
& + \beta x(p_1) x(p_2) (1-Q) \\
& + (1-\alpha-\beta) x(p_1) x(p_2) Q,
\end{aligned}$$

with:

$$\begin{aligned}
B &= \frac{\text{Br}(b \rightarrow \ell)}{\text{Br}(b \rightarrow \ell) + \text{Br}(b \rightarrow X \rightarrow \ell)}, \\
U &= (1-Q) [(1-\chi_B)^2 + \chi_B^2] + 2Q\chi_B(1-\chi_B), \\
L &= (1-Q)2\chi_B(1-\chi_B) + Q[(1-\chi_B)^2 + \chi_B^2], \\
Q &= \frac{1}{2}(1 + q_1 q_2).
\end{aligned}$$

The parameter α is the fraction of $b\bar{b}$ events in the dilepton sample, and β is the fraction of (udsc) dilepton events with opposite charges and is dominated by dileptons from $c\bar{c}$ events.

The B parameter which is the ratio of the efficiency weighted branching ratios is evaluated from the Monte-Carlo events. One finds for muons and electrons the following values:

$$B_\mu = 0.63 \pm 0.01, \quad B_e = 0.84 \pm 0.01.$$

The parameter $C(p_1, p_2)$ takes into account possible correlations between the lepton momenta. This correlation may be induced by photon or gluon emission in the $Z^0 \rightarrow b\bar{b}$ process. This parameter is defined as

$$\begin{aligned}
C(p_1, p_2) &= \exp(-K_t \delta p_{t1} \delta p_{t2}) \\
&\times \exp(-K_\ell \delta p_{\ell 1} \delta p_{\ell 2}),
\end{aligned}$$

where

$$\delta p_{t1} = (p_{t1} - \langle p_{t1} \rangle) / \sigma_{p_t},$$

and

$$\delta p_{\ell 1} = (p_{\ell 1} - \langle p_{\ell 1} \rangle) / \sigma_{p_\ell}.$$

The mono-lepton spectra are used to determine $\langle p_t \rangle$, $\langle p_\ell \rangle$, σ_{p_t} and σ_{p_ℓ} .

A maximum likelihood fit to α , β , χ_B , and K_ℓ and K_t is made. We find $\alpha = 0.88 \pm 0.02$, $\beta = 0.09 \pm 0.02$. K_ℓ and K_t are experimentally compatible with zero. χ_B is determined to be 0.121 ± 0.017 . The likelihood

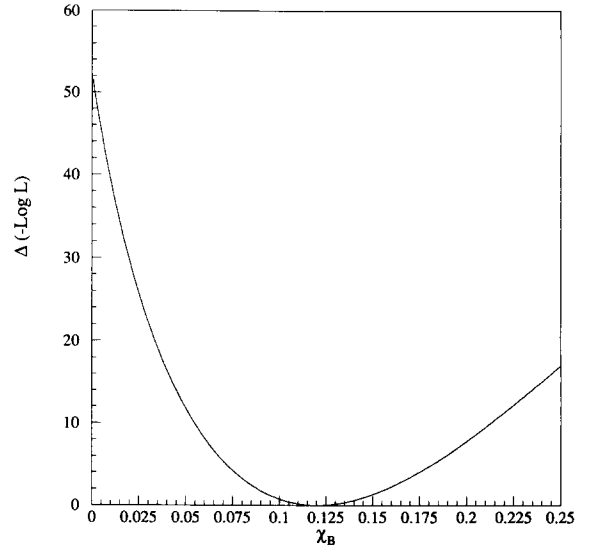


Fig. 2. The likelihood as a function of χ_B for the factorized fit.

as a function of χ_B is shown in fig. 2. As can be seen, the likelihood is asymmetric. Separate fits give $\chi_B = 0.088 \pm 0.024$ for $\mu\mu$, 0.158 ± 0.050 for ee , and 0.140 ± 0.028 for $e\mu$ events.

The systematic errors have been evaluated in a similar manner as in the counting method and are summarized in table 5. We obtain as our final measurement:

$$\chi_B = 0.121 \pm 0.017 \pm 0.006,$$

which is in agreement with the measurements from counting and the four-dimensional fit, as well as with our previous measurement [7] and measurements from other LEP experiments [9,10].

5.4. Discussion of results

To obtain a value of χ_s , a maximum likelihood fit to the data including the results obtained for χ_d has been performed using the relation $\chi_B = f_d \chi_d + f_s \chi_s$. The B_d^0 and B_s^0 fractions, f_d and f_s , are inferred from measurements of the relative production rates of kaons and pions. We have assumed $f_d = 0.40$ and $f_s = 0.12$. These values correspond to a strange quark suppression factor $\gamma_s = f_s/f_d = 0.3$ consistent with measurements at LEP [17] and lower energy e^+e^- colliders [18,19]. The physical constraint, $0 <$

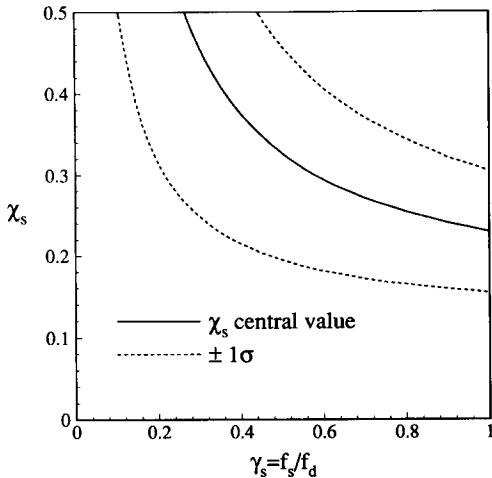


Fig. 3. χ_s as a function of $\gamma_s = f_s/f_d$. The one σ errors include a 50% uncertainty on the value of f_B , the fraction of b-baryons produced.

$\chi_d, \chi_s < 0.5$, was not imposed in the fit which yields $\chi_s = 0.46 \pm 0.21$, consistent with maximal mixing in the $B^0-\bar{B}^0$ system. Imposing the physical constraint $0 < \chi_d, \chi_s < 0.5$ gives the one-dimensional limit at the 90% confidence level of $\chi_s > 0.16$.

The value of χ_s is sensitive to the relative production fractions of different b-hadrons. The dependence of χ_s on γ_s is shown in fig. 3, up to the SU(3) flavor symmetry limit $\gamma_s = 1$. A b-baryon fraction of $f_B = 0.08$ was assumed. The 1σ errors include a 50% uncertainty on the value of f_B . The effect of the uncertainty is a factor 5 smaller than the statistical errors. The value of χ_s is consistent with maximal mixing for any reasonable choice of f_d, f_s and f_B .

6. Conclusions

We have measured mixing in the $B^0-\bar{B}^0$ system using inclusive dilepton events from approximately 410 000 hadronic Z^0 decays. We determine

$$\chi_B = 0.121 \pm 0.017 \pm 0.006.$$

Our result is consistent with maximal mixing in the $B_s^0-\bar{B}_s^0$ system:

$$\chi_s > 0.16$$

at the 90% confidence level.

References

- [1] UA1 Collab., C. Albajar et al., Phys. Lett. B 186 (1987) 247; B 197 (1987) 565(E).
- [2] UA1 Collab., C. Albajar et al., Phys. Lett. B 262 (1991) 171.
- [3] CDF Collab., F. Abe et al., Phys. Rev. Lett. 67 (1991) 3351.
- [4] ARGUS Collab., H. Albrecht et al., Phys. Lett. B 192 (1987) 245.
- [5] CLEO Collab., M. Artuso et al., Phys. Rev. Lett. 62 (1989) 2233.
- [6] ARGUS Collab., H. Albrecht et al., A new determination of the $B^0-\bar{B}^0$ oscillation strength, preprint DESY 92-050, 1992.
- [7] L3 Collab., B.Adeva et al., Phys. Lett. B 252 (1990) 703.
- [8] Mark II Collab., J.F. Kral et al., Phys. Rev. Lett. 64 (1990) 1211.
- [9] ALEPH Collab., D. Decamp et al., Phys. Lett. B 258 (1991) 236; CERN preprint PPE 92/048.
- [10] OPAL Collab., P.D. Acton et al., Phys. Lett. B 276 (1992) 379.
- [11] L3 Collab., B.Adeva et al., Nucl. Instrum. Methods A 289 (1990) 35.
- [12] S. Jezequel, Etude du canal $b \rightarrow e$ et mesure du paramètre de mélange $B^0-\bar{B}^0$ avec le détecteur L3, Ph.D. thesis, L'Université de Savoie (France, 1992).
- [13] T. Sjostrand and M. Bengtsson, Comput. Phys. Commun. 43 (1987) 367; T. Sjostrand, in: Z Physics at LEP1, CERN report CERN-89-08, Vol 3, p. 143.
- [14] The L3 detector simulation is based on GEANT Version 3.14; see R. Brun et al., GEANT 3, CERN DD/EE/84-1 (revised) (September 1987); the GHEISHA program (H. Fesefeldt, RWTH Aachen preprint PITHA 85/02 (1985)) is used to simulate hadronic interactions.
- [15] Particle Data Group, J.J. Hernández et al., Review of particle properties, Phys. Lett. B 239 (1990) VII.113, we have averaged the PETRA and PEP measurements according to the procedure used by the Particle Data Group.
- [16] L3 Collab., B.Adeva et al., Phys. Lett. B 261 (1991) 177.
- [17] OPAL Collab., G. Alexander et al., Phys. Lett. B 264 (1991) 467.
- [18] JADE Collab., W. Bartel et al., Z. Phys. C 20 (1983) 187.
- [19] TASSO Collab., M. Althoff et al., Z. Phys. C 27 (1985) 27.